The Refined Structure of the ϵ-Aminocaproic Acid Complex of Human Plasminogen Kringle 4[†,‡]

Tswei-Ping Wu, Kaillathe Padmanabhan, A. Tulinsky,* and Anne M. Mulichak[§]

Department of Chemistry, Michigan State University, East Lansing, Michigan 48824

Received April 15, 1991; Revised Manuscript Received July 23, 1991

ABSTRACT: The crystallographic structure of the plasminogen kringle 4–ϵ-aminocaproic acid (ACA) complex (K4–ACA) has been solved by molecular replacement rotation–translation methods utilizing the refined apo-K4 structure as a search model (Mulichak et al., 1991), and it has been refined to an R value of 0.148 at 2.25-Å resolution. The K4–ACA structure consists of two interkringle residues, the kringle along with the ACA ligand, and 106 water molecules. The lysine-binding site has been confirmed to be a relatively open and shallow depression, lined by aromatic rings of Trp62, Phe64, and Trp72, which provide a highly nonpolar environment between doubly charged anionic and cationic centers formed by Asp55/Asp57 and Lys35/Arg71. A zwitterionic ACA ligand molecule is held by hydrogen-bonded ion pair interactions and van der Waals contacts between the charged centers. The lysine-binding site of apo-K4 and K4–ACA have been compared: the rms differences in main-chain and side-chain positions are 0.25 and 0.69 Å, respectively, both practically within error of the determinations. The largest deviations in the binding site are due to different crystal packing interactions. Thus, *the lysine-binding site appears to be preformed*, and lysine binding does not require conformational changes of the host. The results of NMR studies of lysine binding with K4 are correlated with the structure of K4–ACA and agree well.

Plasmin, a trypsin-like serine protease, is primarily responsible for the removal of fibrin deposits from the walls of blood vessels. Plasmin generation takes place predominantly when and where fibrin formation occurs (Wiman & Collen, 1978). Both PG[1] and TPA are adsorbed on fibrin with the aid of their lysine-binding sites to form a ternary complex; activation of PG then occurs within the complex (Holyaerts et al., 1982). The plasmin formed remains bound to fibrin polymer, degrading fibrin into soluble fragments and thus removing the fibrin deposit.

The interactions between plasmin, PG, and TPA with fibrin are located in specific domains, three of which are structural and functional folding domains with three-disulfide triple-loop patterns called kringles (Magnusson et al., 1975). Kringles are found repeatedly among proteins which are involved in blood coagulation and fibrinolysis [see Mulichak et al. (1991) for a summary]: K2 of TPA (van Zonneveld et al., 1986) and K1 and K4 of PG (Lerch et al., 1980; Trexler et al., 1982) additionally bind to fibrin, lysine, or ω-aminocarboxylic acids in general (Winn et al., 1980) and ACA in particular. Chemical modifications of K4 have been carried out (Trexler et al., 1982) which showed that residues Asp57 and Arg71 (Figure 1) are directly involved in ligand binding. This enabled the lysine-binding subsite region of fibrin-binding kringles to be described in three dimensions (Tulinsky et al., 1988a) on the basis of the folding and tertiary structure of PTF1 (Park & Tulinsky, 1986; Tulinsky et al., 1988b) which additionally implied that Asp55 might be important. The binding subsite structure was subsequently confirmed with the crystallographic structure determination of human PGK4 (Mulichak & Tulinsky, 1990; Mulichak et al., 1991). However, a cofacial intermolecular interaction between the binding sites of neighboring molecules excluded access of the site to small molecule ligands like ACA by diffusion into crystals, precluding the formation of the K4–ACA complex thusly. This led us to crystallize PGK4 in the presence of ACA ligand. We report here a 2.25-Å resolution X-ray crystallographic structure of the human K4–ACA complex which reveals the manner of lysine binding. The structure is also compared with the 1.9-Å resolution refined structure of human apo-PGK4 (Mulichak et al., 1991).

Materials and Methods

Crystals of K4–ACA were grown by the sitting drop method using 30% PEG 8000, 0.12 M ammonium sulfate, pH 6.0, and 1.4% DMF in the presence of 25 mM ACA. Although the conditions were practically the same as those which produce orthorhombic apo-K4 crystals, K4–ACA crystallizes in the monoclinic space group $P2_1$ with unit cell dimensions a = 42.21 Å, b = 35.46 Å, c = 25.43 Å, β = 102.9°, two molecules per unit cell, 65.5% protein fraction and V_m = 1.89 Å^3/dalton (Matthews, 1968). Most of the crystals have a plate-shaped form; the crystal used for intensity data collection had dimensions of 0.8 × 0.4 × 0.2 mm. Probably due to the high protein content, the crystals proved to be practically insensitive to damage due to X-ray exposure. Three-dimensional intensity data were measured to 2.25-Å resolution (3198 reflections observed greater than twice the magnitude of the average value of negative intensities of 3381 measured of about 3400 possible, 95%) using a Wyckoff stepscan procedure (Wyckoff et al., 1967) with a Nicolet P3/F diffractometer. The intensity data were corrected for absorption (North et al., 1968) and intensity decay with X-ray exposure using procedures similar to those

[†] This work was supported by NIH Grant HL25942.

[‡] The atomic coordinates of the complex have been deposited in the Brookhaven Protein Data Bank.

* To whom inquiries should be addressed.

[§] Present address: The Upjohn Company, Kalamazoo, MI 49001.

[1] Abbreviations: PG, plasminogen; TPA, tissue-type plasminogen activator; K1, K2, etc., kringle 1, kringle 2, etc.; ACA, ϵ-aminocaproic acid; PT, prothrombin; F1, fragment 1; K4–ACA, ACA complex of K4; DMF, dimethyl formamide; AMCHA, *trans*-(4-aminomethyl)cyclohexanecarboxylic acid.

0006-2960/91/0430-10589$02.50/0

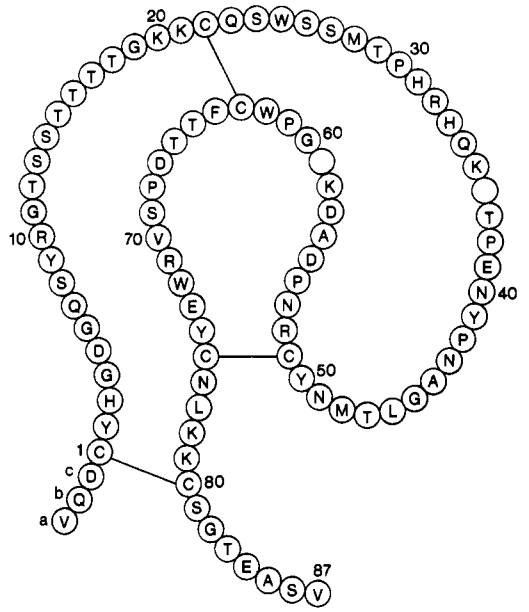

FIGURE 1: Sequence of human plasminogen kringle 4. Interkringle peptide residues are between a–c and 81–87. The numbering is based on the PGK5 convention.

described elsewhere (Tulinsky et al., 1985; Mulichak et al., 1991).

The K4–ACA structure was solved by molecular replacement rotation–translation methods utilizing the refined PGK4 structure as a search model (Mulichak et al., 1991). The rotation search was performed in Patterson space (1500 largest peaks, 8.0–3.0-Å shell, 1408 reflections, vectors between 3.0 and 15 Å) with the SEARCH routine in the program PROTEIN (Steigemann, 1974). The highest rotation peak was 7.4σ above the background, with the next highest peak at 5.3σ. The position of the model in the unit cell after rotation to the former orientation was found using the program BRUTE (Fujinaga & Read, 1987) by a translation search first in 0.5- then 0.1-Å increments with data from 8.0–3.0-Å resolution and simply searching in the xz plane. The highest peak had a correlation coefficient of 0.43 (about 16σ above the mean). An electron density map based on this rotation–translation position clearly revealed the K4 structure and, in addition, new electron density extending between the side chains of Asp57 and Arg71.

The starting PGK4 model of K4–ACA was refitted using interactive computer graphics with the program FRODO (Jones, 1982). The structure was then refined employing the restrained least-squares method implemented in the program PROFFT (Finzel, 1987) with intermittent model building performed on an Evans and Sutherland PS390 interactive stereographics. The refinement proceeded in stages, each of which was followed by model building using ($2|F_o| - |F_c|$) and ($|F_o| - |F_c|$) maps and the examination of the Ramachandran plot. The initial R value started at 0.43 with an overall thermal parameter of 16 Å^2; R decreased to 0.26 after the first stage (2.8-Å resolution). As phases improved, higher resolution data were added to 2.5-Å resolution. The unaccounted for density between Asp57 and Arg71 now appeared convincingly to be due to ACA. Therefore, an ACA was fitted into the density and included in the refinement. Water molecules were also gradually added. Peaks were considered to be possible water molecules when they were above a 2.8σ threshold and common to both (7.0 – 2.5) Å and (8.0 – 2.5)Å resolution difference maps. Of these, peaks were selected as water for structure factor calculations only if they were within 2.5–4.0 Å of the protein or another water molecule. New water molecules included into the refinement were initially assigned an occupancy of 0.75 and an overall B obtained from the last refinement stage. The B values of the water molecules were refined first followed by occupancies. In the last stages of refinement, the remainder of the data (to 2.25 Å) were included, and reflection weights were assigned in seven shells of sin θ/λ based on $\langle||F|_o - |F|_c|\rangle/2$ of the range. The final reflection weights and R values in each range are given in Table I, and a summary of refinement parameters is listed in Table II. The final K4–ACA structure has a crystallographic R value of 0.148 for 2993 reflections between 7.0- and 2.25-Å resolution with 106 water molecules and an average thermal parameter of 17.9 Å^2. The average occupancy of the water molecules is about 0.75, and their average thermal parameter (19 Å^2) is slightly higher than that of the protein (17.5 Å^2). An estimate of the mean error in coordinates suggests a value of about 0.2 Å.

Table I: Weights of Reflections and R Values of the Final Refinement

D_{min} (Å)	no. reflections	$\sigma(\|F\|)^a$	$\langle\|\|F_o\| - \|F_c\|\|\rangle$	R value shell	R value sphere
4.00	465	11.2	25.6	0.153	0.153
3.30	465	9.9	19.2	0.124	0.139
2.90	493	9.1	16.0	0.150	0.142
2.60	555	8.4	14.1	0.157	0.145
2.45	375	7.8	13.5	0.171	0.148
2.35	288	7.5	11.5	0.151	0.148
2.25	352	7.2	11.0	0.148	0.148

^{a} $\sigma(|F|) = 18.0 - 70.0(\sin\theta/\lambda - 1/6)$.

Table II: Summary of Final Least-Squares Parameters and Deviations

	target σ	rms Δ
distances (Å)		
bond distance	0.015	0.017
angle distance	0.025	0.042
planar 1, -4 distance	0.035	0.050
nonbonded distances (Å)		
single torsion	0.50	0.20
multiple torsion	0.50	0.32
possible H-bond	0.50	0.32
torsion angles (deg)		
planar	3	4
staggered	15	23
orthonormal	20	16
plane groups (Å)	0.02	0.02
chiral centers (Å^3)	0.13	0.23
thermal restraints (Å^2)		
main-chain bond	1.5	1.8
main-chain angle	2.0	2.6
side-chain bond	2.5	2.3
side-chain angle	2.5	3.6
av angle = 116.8 ± 2.3°		

Results and Discussion

General. The refined K4–ACA structure extends from residue Gln-b to Cys80 (Figure 1) along with the ACA ligand; there was no electron density for the N-terminal Val-a nor for the C-terminal interkringle pentapeptide. A similarly disordered interkringle region was found in the apo-K4 structure (Mulichak et al., 1991) and might be due in part to the interkringle link heterogeneity discussed there. There was also only little electron density for the Thr18 and Arg32 side chains; therefore, they were refined as alanines. The distribution of main-chain torsion angles (ϕ,ψ) is shown in Figure 2, from

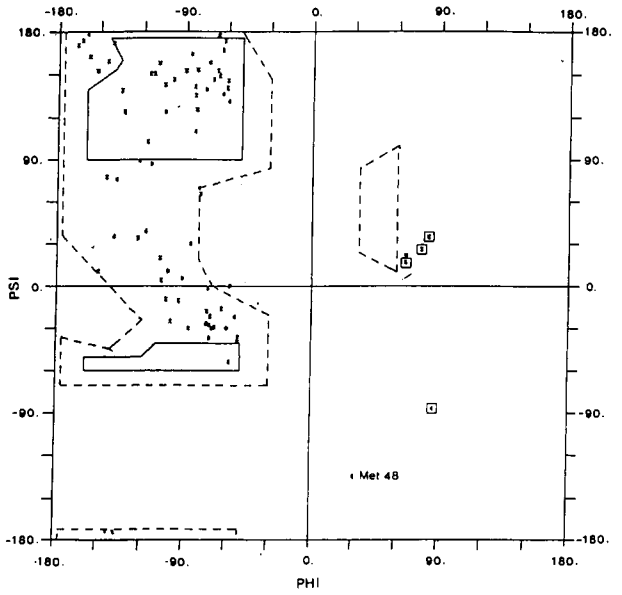

FIGURE 2: Ramichandran plot of final ϕ,ψ angles of K4–ACA. The Gly residues are boxed.

which it can be seen that all the residues conform well with allowed regions except for one outlier (Met48); however, the latter fits in very well-defined electron density and has the same conformation as that observed in apo-K4 (Mulichak et al., 1991). Moreover, a *cis*-proline was found at position 30, similar to the apo-K4 structure. Conversely, in K4–ACA the sulfur atom of Cys75 is localized in one position while it was distributed between two different equally occupied positions in the apostructure giving rise to different disulfide conformations (Mulichak et al., 1991). The localization in K4–ACA could be a result of ACA ligand binding or possibly due to different packing in the crystal structure. The average thermal parameter of the kringle in K4–ACA is 17.5 Å^2, but although the electron density of the ACA is quite good (Figure 3), it has an average *B* value which is about twice that of the kringle (34 Å^2). Since the ACA is fixed in the lysine-binding site by two doubly charged, hydrogen-bonding, ion pair interactions, the higher *B* value of ACA must reflect a microheterogeneity of its positioning within the binding site similar to that observed for hirudin in its complex with α-thrombin (Rydel et al., 1991).

Of the hydrogen-bond interactions in the K4–ACA structure, all but eight are also common to the apo-K4 structure (Mulichak et al., 1991); the ones present in K4–ACA and not in apo-K4 are listed in Table III. The criteria used to identify possible hydrogen bonds were (a) a donor–acceptor center distance of less than 3.05 Å and (b) a hydrogen-bond angle of greater than 120°. Of the new hydrogen bonds, the Gln7N–Asp5OD2 is borderline, the Tyr9OH–AspcOD1 involves an interkringle residue which was disordered in the apostructure, the Lys20NZ–Glu73OE1 makes the only ion pair of K4 a hydrogen-bonded one, and the hydrogen bond between Arg71NH1 and Arg32O just satisfies the selection criteria. Also listed in Table III are two apparently important hydrogen bonds involving Asp55/Asp57 of the lysine-binding site of both structures, which will be addressed later.

Lysine-Binding Site. The lysine-binding site is a relatively open, elongated, shallow depression located on the kringle surface that is formed by His31–Lys35, Pro54–Lys58, Pro61–Phe64, and Arg71–Cys75 (Figure 4). At neutral pH, there are two negatively charged residues located on one end of the binding site (Asp55 and Asp57) with carboxylate oxygens 5.2 Å from one another; there are also two positively charged residues located at the other end of the depression

Table III: New Intramolecular Hydrogen Bonds of K4–ACA[a]

donor	acceptor	distance (Å) D···A	distance (Å) H···A	angle (deg) DHA	angle (deg) CAH
Gln7 N	Asp5 OD2	3.08	2.22	145	156
Tyr 9 OH	Aspc OD1	2.63	1.69	156	104
Arg10 NH2	Asn43 O	2.89	2.30	118	157
Lys20 NZ	Glu73 OE1	2.96	2.17	132	152
Ser27 OG	Thr29 O	2.74	1.99	134	123
Thr37 N	Gln34 O	2.89	2.02	142	101
Thr47 N	Gly45 O	2.71	1.86	137	103
Arg71 NH1	Arg32 O	3.01	2.17	143	139
Trp62 NE1	Asp55 OD2	2.99	2.43	116	120
Tyr74 OH	Asp57 OD2	2.59	1.71	152	105

[a] D = donor; A = acceptor.

Table IV: Hydrogen Bonds between K4 and ACA

donor	acceptor	distance (Å) D···A	distance (Å) H···A	angle (deg) DHA	angle (deg) CAH
Lys35 NZ	ACA O1	2.72	1.99	127	148
Arg71 NE	ACA O2	2.71	1.83	145	147
Arg71 NH2	ACA O2	2.89	2.09	134	129
ACA NZ	Asp57 OD1	2.84	2.28	113	107
ACA NZ	Asp55 OD2	2.12	1.97	84	112

(Lys35 and Arg71) with quaternary amino groups 6.3 Å from one another. Thus, the binding site contains doubly charged anionic and doubly charged cationic centers as previously inferred (Mulichak et al., 1991). The depression, lined by aromatic rings of Trp62, Phe64, and Trp72, also provides a highly nonpolar environment between the charged centers so that the lysine-binding site approximates a dipolar surface as first suggested from modeling (Tulinsky et al., 1988a). Thus, zwitterionic ligands such as lysine and ACA can first interact at long range in preparation of docking, ultimately being anchored by ion pair interactions. The close van der Waals contacts between the methylene carbons of ligand and the aromatic residues between the charge centers additionally assist the binding.

Kringle 4–ACA Interaction. A zwitterionic ACA molecule in an extended conformation lies between the doubly charged anionic and cationic centers of K4 formed by Asp55/Asp57 and Lys35/Arg71 (pH of crystals is 6.0), which also makes four or five hydrogen bonds with these residues (Table IV) and interacts with the lipophilic core formed by Trp62, Phe64, and Trp72 through the methylenes between the zwitterionic charges (Figure 3 and 4). The hydrogen bond to Asp55 is questionable since its donor–acceptor angle is so small; however, its ion pair interaction is undeniable and even appears to be stronger than that of Asp57. The oxygen atoms of the carboxylate groups of Asp55 (OD2) and Asp57 (OD2) are hydrogen bonded back to the kringle (Table III), which might aid in aligning and anchoring the side chains for ligand binding. The Asp57 and Arg71 residues were originally implicated in ligand binding through modification of Asp57 with 1-ethyl-3-(3-dimethylaminopropyl)carbodiimide and Arg71 with 1,2-cyclohexanedione (Trexler et al., 1982), while the participation of Asp55 was suggested on the basis of computer modeling (Tulinsky et al., 1988a). However, from Figures 3 and 4 and Table IV, it is clear that Lys35 also participates as an integral member of the principal binding residues as inferred from the apo-K4 structure (Mulichak & Tulinsky, 1990; Mulichak et al., 1991) and in agreement with modification studies which showed that blocking Lys35 decreases the affinity of K4 for lysine–Sepharose (Trexler et al., 1985). Computer modeling also suggests a doubly charged cationic

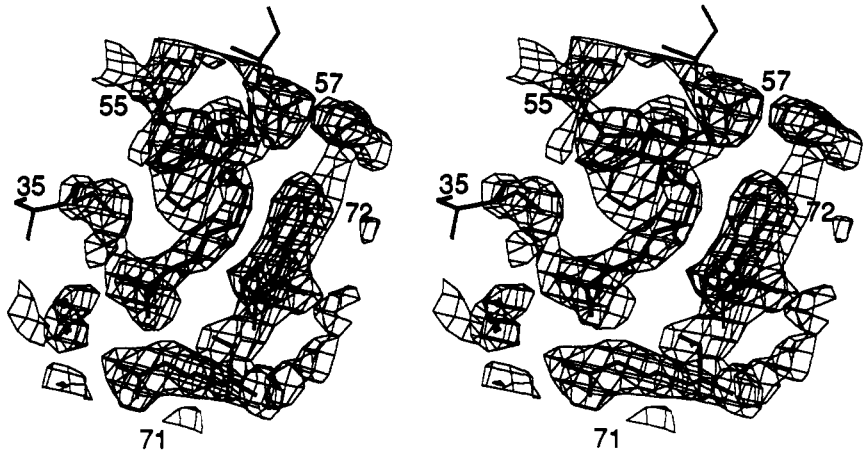

FIGURE 3: Stereoview of the electron density of the lysine-binding site of K4–ACA. ACA is located between Asp55/Asp57 and Lys35/Arg71; the basket contour is at 1σ.

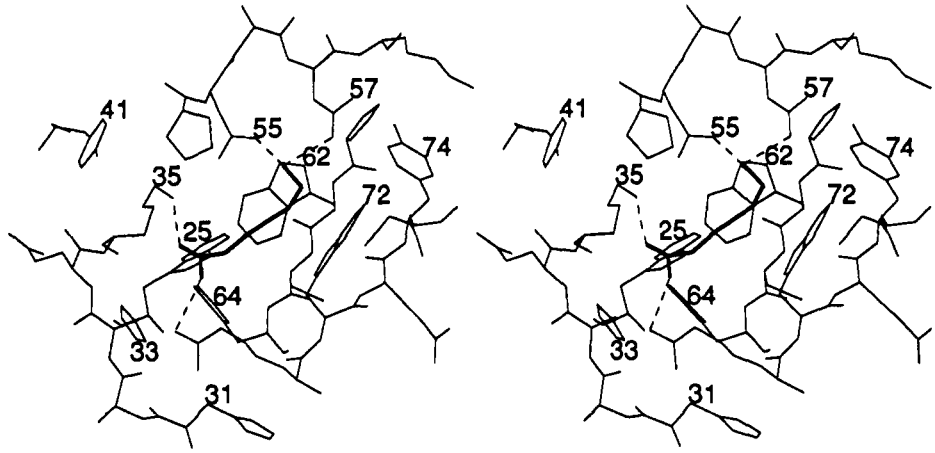

FIGURE 4: Stereoview of the lysine-binding site of K4–ACA. ACA is shown in bold; hydrogen bonds are dashed.

center in the binding site of PGK1 involving Arg34 and Arg71 (Tulinsky et al., 1988a). In the case of K4, the guide coordinates for modeling Lys35 had to be based on Ile35 of PTF1, which only extended to CB, so that the lysyl side chain was simply modeled in an extended energy-minimized conformation. This is clearly not the case as Lys35 retreats toward Arg71 in the binding site and gives rise to a doubly charged center in both the apo- and K4–ACA structures. The new finding thus places the K4 binding site on a comparative level to modeled PGK1 with respect to a doubly charged positive center.

Comparison of K4–ACA and Apo-K4 Structures. The structures of PGK4 and PTK1 have already been compared elsewhere (Mulichak & Tulinsky, 1990), which showed that the lysine-binding site is approximated fairly well by PTK1 but with some notable exceptions. These render PTK1 to be a nonbinding kringle. The structure of PGK4 has additionally been compared here with the K4–ACA structure by the optimal superpositioning of CA, C, and N atoms. The rms differences between the two structures are listed in Table V. The agreement between the two structures is good for the main-chain atoms and superb (0.27 Å) after removing about 15% of the atoms having deviations greater than 1σ. The differences between the apo and the complexed structure in the lysine-binding site are listed in Table VI and a stereoview of the superposition of the binding site regions is shown in Figure 5. The average rms difference in main-chain position in the site is only 0.25 Å with only one difference as large as 0.50 Å, while the average of the side groups is 0.69 Å. The largest deviations in the binding site are due to crystal packing interactions. In the K4–ACA structure, Gln34 forms a hydrogen bond with the carbonyl oxygen of Trp72 of a neighboring molecule, giving rise to a rms deviation of 1.12 Å. Other significant deviations occur with Asp55 and Asp57 of the anionic charge center (0.75 and 1.23 Å, respectively). These are the consequence of a cofacial kringle–kringle interaction of the binding site regions of two neighboring molecules in the apo-K4 structure (Mulichak et al., 1991). The Asp55/Asp57 of one molecule form two ion pairs with Arg32/Arg71 of neighboring molecules; thus, Asp55 and Asp57 in apo-K4 point somewhat away from the lipophilic binding core, which leads to relatively large deviations from the K4–ACA structure. It is also noteworthy that Arg32 appears to be disordered in K4–ACA where it cannot make a similar intermolecular interaction. In the case of Lys58, it is involved in a complex intermolecular interaction in the apostructure with a sulfate ion of a neighboring molecule (Mulichak et al., 1991). Interestingly, the position of the sulfate anion in K4 is close to the cationic center in K4–ACA (Figure 5). Lastly, the side chain of Lys35 in apo-K4 forms a hydrogen-bonding ion pair with the sulfate thus making the side-chain conformation a little different from that of the cationic center in K4–ACA (Table VI). The remainder of the residues in the lysine-binding site are practically identical in the two structures. Thus, from all appearances, *the lysine-binding pocket is preformed* in the kringle structure, and ACA binding takes place without requiring any conformational changes of the host.

Ligand Interactions and NMR. The indole side chains of Trp62 and Trp72 form end-to-face contacts with the rings of

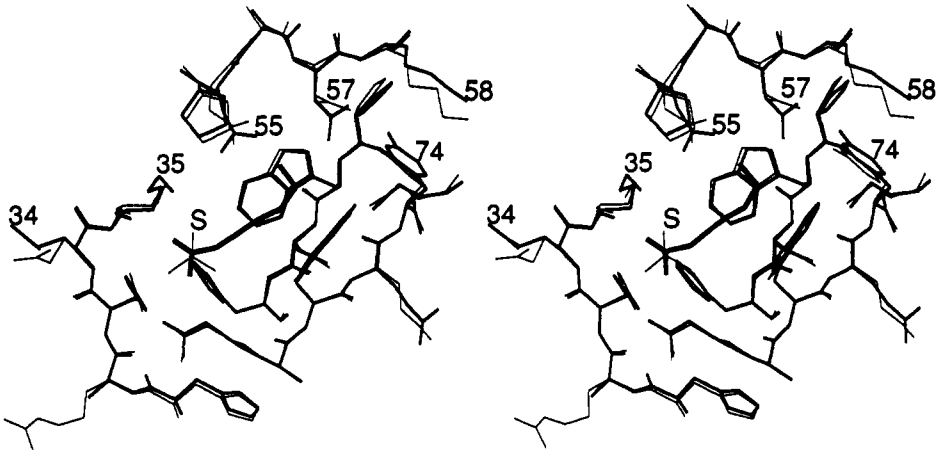

FIGURE 5: Stereoview of the comparison of the lysine-binding site of K4–ACA and Apo-K4. K4–ACA is in bold; the sulfate position in apo-K4 is designated by S.

Table V: RMS Difference between the K4–ACA and Apo-K4

	Δ (Å)	atoms[a]
all protein atoms	0.57	602
main chain	0.44	237
carbonyl oxygens	0.60	79
side chains	0.66	286
sulfurs (Cys, Met)	0.44	8
α-carbon	0.43	79

[a] Number of atoms in the comparison.

Table VI: Differences in Lysine-Binding Sites between K4–ACA and Apo-K4

residue	rms Δ (Å) (main chain)	rms Δ (Å) (side chain)
His31	0.21	0.28
Arg32	0.17	0.50
His33	0.16	0.19
Gln34	0.23	1.12
Lys35	0.26	0.70
Pro54	0.36	0.23
Asp55	0.19	0.75
Ala56	0.50	0.35
Asp57	0.25	1.23
Lys58	0.25	1.27
Pro61	0.10	0.54
Trp62	0.26	0.20
Cys63	0.19	0.35
Phe64	0.15	0.12
Arg71	0.10	0.21
Trp72	0.23	0.44
Glu73	0.19	0.65
Tyr74	0.10	0.53
Cys75	0.20	0.29
av rms	0.25	0.69

Phe64 and Tyr74, respectively (Figure 4); such aromatic clustering is common in proteins and provides enhanced stability (Burley & Petsko, 1985) to the hydrophobic depression. NMR NOE experiments (Ramesh et al., 1987; Andrew et al., 1989) found that the side chains of Trp62, Phe64, and Trp72 are perturbed most by ligand presence and that Trp25, His31, His33, Tyr41, and Tyr74 are also affected, but to a lesser extent. This agrees well with the crystal structure. Most of these aromatic residues are near the surface in the binding site region within which the ligand lies in an extended conformation (Figures 3 and 4). The ring of Phe64 is as close as 3.2 Å from CA of ACA and approximately 3.9 Å from the end of the Trp62 indole ring; thus, it appears that the phenylalanyl ring can be affected through the aromatic stacking interaction with the Trp62 side chain or possibly by a substitution at the CA position of ligand. This conforms with Phe64 having large ligand-induced chemical shifts with such ligands (Andrew et al., 1989). Although somewhat removed from the binding center, the tyrosyl ring of Tyr74 is positioned 3.7 Å from the end of the indole of Trp72 while its hydroxyl group appears to be making an important hydrogen bond orienting the carboxylate group of Asp57. The Tyr74 may sense ligand-binding effects indirectly from the aromatic interaction with Trp72 and/or the hydrogen-bonding interaction with Asp57. The His33 residue, which is at the perimeter of the binding site, has its imidazole ring stacked parallel to the phenyl ring of Phe64 and within 4.5 Å. The binding of bulkier ligands such as AMCHA may have a greater influence on this imidazole ring. In contrast to His33, His31 is located away from the binding core and ligand in agreement with NMR observations which show that it only has a small chemical shift upon ligand binding (Ramesh et al., 1987; Andrew et al., 1989). The indole ring of Trp25 is in the next layer below the surface, but its end is oriented about 4.0 Å from the face of the indole of Trp62. It also displays only minor ligand effects which most likely transmit through the aromatic–aromatic interaction with Trp62; however, it too may experience greater effects from bulkier ligands. Lastly, the side chain of Tyr41 is located distantly from the center of the binding site. Therefore, it can only sense the presence of ligand through secondary effects transmitted through residues in the immediate vicinity of the ligand.

ACKNOWLEDGMENTS

We thank Dr. Miguel Llinas for providing us with samples of PGK4 and ACA.

Registry No. Lys, 56-87-1.

REFERENCES

Andrew, M., Ramesh, V., & Llinas M. (1989) *Biochemistry 28*, 1368–1376.
Burley, S. K., & Petsko, G. A. (1985) *Science 229*, 23–28.
Finzel, B. C. (1987) *J. Appl. Crystallogr. 20*, 53–55.
Fujinaga, M., & Read, R. J. (1987) *J. Appl. Crystallogr. 20*, 517–521.
Hoylaerts, M., Rijken, D. C., Lijnen, H. R., & Collen, D. (1982) *J. Biol. Chem. 257*, 2912–2919.
Jones, T. A. (1982) in *Computational Crystallography* (Sayre D., Ed.) pp 303–317, Clarendon Press, Oxford.

Lerch, P. G., Rickli, E. E., Lergier, W., & Gillessen, D. (1980) *Eur. J. Biochem. 107*, 7–13.

Magnusson, S., Petersen, T. E., Sottrup-Jensen, L., & Claeys, H. (1975) in *Proteases and Biological Control* (Reich, E., Rifkin, D. B., & Shaw, E., Eds.) pp 123–149, Cold Spring Harbor Laboratories, Cold Spring Harbor, NY.

Matthews, B. W. (1968) *J. Mol. Biol. 33*, 491–497.

Mulichak, A. M., & Tulinsky, A. (1990) *Blood Coagulation Fibrinolysis 1*, 673–679.

Mulichak, A. M., Park, C. H., Tulinsky, A., & Llinas, M. (1989) *J. Biol. Chem. 264*, 1922–1923.

Mulichak, A. M., Tulinsky, A., & Ravichandran, K. G. (1991) *Biochemistry* (preceding paper in this issue).

North, A. C. T., Philips, D. C., & Matthews, F. S. (1968) *Acta Crystallogr. 24A*, 351–359.

Park, C. H., & Tulinsky, A. (1986) *Biochemistry 25*, 3977–3982.

Ramesh, V., Petros, A. M., Llinas, M., Tulinsky, A., & Park, C. H. (1987) *J. Mol. Biol. 198*, 481–498.

Rydel, T. J., Tulinsky, A., Bode, W., & Huber, R. (1991) *J. Mol. Biol.* (in press).

Steigemann, W. (1974) Ph.D. Dissertation, Technische Universitat, Munchen.

Trexler, M., Vali, Z., & Patthy, L. (1982) *J. Biol. Chem. 257*, 7401–7406.

Trexler, M., Banyai, L., Patthy, L., Pluck, N. D., & Williams, R. J. P. (1985) *Eur. J. Biochem. 152*, 439–446.

Tulinsky, A., Park, C. H., & Rydel, T. J. (1985) *J. Biol. Chem. 260*, 10771–10778.

Tulinsky, A., Park, C. H., Mao, B., & Llinas, M. (1988a) *Proteins 3*, 85–96.

Tulinsky, A., Park, C. H., & Jankun, E. (1988b) *J. Mol. Biol. 202*, 885–901.

van Zonneveld, A. J.; Veerman, H., & Pannekoek, H. (1986) *Proc. Natl. Acad. Sci. U.S.A. 86*, 4670–4674.

Wiman, B., & Collen, D. (1978) *Nature (London) 272*, 549–550.

Winn, E. S., Hu, S.-P., Hochschwender, S. M., & Laursen, R. A. (1980) *Eur. J. Biochem. 104*, 579–586.

Wyckoff, H. W., Doscher, M., Tsernoglou, D., Inagami, T., Johnson, L. N., Hardman, K. D., Allewell, N. M., Kelly, D. M., & Richards, F. M. (1967) *J. Mol. Biol. 27*, 563–578.